Practical Considerations For Passive Reduction of RLC Circuits

Altan Odabasioglu and Mustafa Celik
{altan, celik}@montereydesign.com
Monterey Design Systems, Inc.
Sunnyvale, CA 94089

Lawrence T. Pileggi
pileggi@ece.cmu.edu
Department of Electrical and Computer Engineering
Carnegie Mellon University
Pittsburgh, PA 15213

Abstract

Krylov space methods initiated a new era for RLC circuit model order reduction. Although theoretically well-founded, these algorithms can fail to produce useful results for some types of circuits. In particular, controlling accuracy and ensuring passivity are required to fully utilize these algorithms in practice. In this paper we propose a methodology for passive reduction of RLC circuits based on extensions of PRIMA, that is both broad and practical. This work is made possible by uncovering the algebraic connections between this passive model order reduction algorithm and other Krylov space methods. In addition, a convergence criteria based on an error measure for PRIMA is presented as a first step towards intelligent order selection schemes. With these extensions and error criterion, examples demonstrate that accurate approximations are possible well into the RF frequency range even with expansions about s=0.

1. Introduction

The objective of model order reduction is to replace the original linear circuit with a reduced mathematical description that retains sufficient information about the original circuit. This is obtained by matching certain characteristics - such as moments- of the original circuit to the reduced order model.

The smooth transfer functions in RC circuits allowed direct moment matching methods such as AWE [1] to be applied successfully. However, these methods often fail to supply enough accuracy for RLC circuits, particularly because of the noise associated with matching moments directly. With the use of Krylov subspace methods, it has been possible to obtain very high order approximations [2, 3, 4, 5] since the moments are computed with less numerical noise and matched implicitly.

PRIMA (Passive Reduced-order Interconnect Macromodeling Algorithm) [6] was introduced recently as a Krylov space method which provides passive, stable macromodels with accuracy comparable to the most accurate reduction techniques. However, while the algorithms in [6] are theoretically correct, an implementation based on this description is not robust. In this paper, we have developed a robust framework based on PRIMA by unveiling the connections between this passive reduction technique and other well-known Krylov space based processes; even those that fail to satisfy passivity and/or stability requirements. Examples demonstrate that the flexibility supplied by this methodology results in better accuracy and robustness even with moment expansions around s=0. The methodology and problems for the RC circuits are also discussed as a special case.

Obtaining better accuracy and smaller macromodel size is the goal in the reduction process. Unfortunately, these objectives are often contradictory. Given a maximum frequency of interest, there exists a minimum order of approximation, $q_{\min}$ that will satisfy this requirement. If the order is less than $q_{\min}$, it means that the macromodel is not accurate enough. On the other hand, if it is more than $q_{\min}$, the size of the macromodel is larger than needed, which impacts the final simulation time.

Without a reliable order selection mechanism, human interaction is required, making model-order reduction less practical for certain applications. To determine the order of approximation, reliable error measures are needed. A PRIMA accuracy measure based on the residual error has been developed in [7]. The residual error concept is used in iterative system solutions [8] but it may not reflect the frequency domain behavior for the exact error. Recently PVL-WEB [9] showed an error measure that is an approximation to the exact error for the PVL [2] algorithm; however its region of validity was limited. Following similar principles, we derive a robust error criterion for PRIMA, that does not have a similar region of validity problem. The use of this error measure as a convergence criterion is successfully demonstrated.

2. Background

To obtain the admittance matrix of a multiport, voltage sources are connected to the ports. The multiport, along with these sources, constitutes the Modified Nodal Analysis (MNA) equations:

$$\begin{aligned} \mathbf{C}\,\dot{\mathbf{x}}_n &= -\mathbf{G}\,\mathbf{x}_n + \mathbf{B}\,\mathbf{u}_p \\ \mathbf{i}_p &= \mathbf{L}^T\,\mathbf{x}_n \end{aligned} \tag{1}$$

The $\mathbf{i}_p$ and $\mathbf{u}_p$ vectors denote the port currents and voltages respectively and

*This work was funded in part by the National Science Foundation and Monterey Design Systems.

 0-7803-5832-X /99/$10.00 ©1999 IEEE.

$$\mathbf{G} \equiv \begin{bmatrix} \mathbf{N} & \mathbf{E} \\ \mathbf{E}^T & \mathbf{0} \end{bmatrix} \qquad \mathbf{C} \equiv \begin{bmatrix} \mathbf{Q} & \mathbf{0} \\ \mathbf{0} & -\mathbf{P} \end{bmatrix} \qquad \mathbf{x}_n \equiv \begin{bmatrix} \mathbf{v} \\ \mathbf{i} \end{bmatrix} \tag{2}$$

where $\mathbf{v}$ and $\mathbf{i}$ are the MNA variables corresponding to the node voltages, inductor and voltage source currents respectively. $\mathbf{G} \in \Re^{nxn}$ and $\mathbf{C} \in \Re^{nxn}$ represent the conductance and susceptance matrices. $\mathbf{N}$, $\mathbf{Q}$ and $\mathbf{P}$ are the matrices containing the stamps for resistors, capacitors and inductors respectively. $\mathbf{E}$ consists of ones, minus ones and zeros, which represent the current variables in KCL equations. Note that $\mathbf{G}$ and $\mathbf{C}$ are symmetric and non-definite matrices.

The original PRIMA implementation [6] consisted of these three separate stages:

1) Negated stamping of $\mathbf{G}$ to make $\mathbf{G}_{pr}$ and $\mathbf{C}_{pr}$ positive semi-definite for RLC circuits. Define a transformation matrix,

$$\mathbf{T} = \begin{bmatrix} \mathbf{I} & \mathbf{0} \\ \mathbf{0} & -\mathbf{I} \end{bmatrix} \tag{3}$$

$$\text{such that } \mathbf{G}_{pr} = \mathbf{TG} = \begin{bmatrix} \mathbf{N} & \mathbf{E} \\ -\mathbf{E}^T & \mathbf{0} \end{bmatrix} \text{ and } \mathbf{C}_{pr} = \mathbf{TC} = \begin{bmatrix} \mathbf{Q} & \mathbf{0} \\ \mathbf{0} & \mathbf{P} \end{bmatrix} \tag{4}$$

are positive semi-definite matrices. $\mathbf{T}$ is never constructed explicitly, since it is rather easy to implement the same transformation during stamping.

2) The Arnoldi Algorithm to find the orthogonal Krylov subspace spanning vectors, $\mathbf{X}$. The Krylov space is defined as

$$Kr(\mathbf{A}, \mathbf{R}, k) \equiv colsp[\mathbf{R}, \mathbf{AR}, \mathbf{A}^2\mathbf{R}, \ldots, \mathbf{A}^k\mathbf{R}] \tag{5}$$

$$\text{where } \mathbf{A} \equiv -\mathbf{G}^{-1}\mathbf{C} \text{ and } \mathbf{R} \equiv \mathbf{G}^{-1}\mathbf{B}. \tag{6}$$

3) The congruence transformations to obtain reduced system,

$$\tilde{\mathbf{C}} = \mathbf{X}^T\mathbf{C}_{pr}\,\mathbf{X} \qquad \tilde{\mathbf{G}} = \mathbf{X}^T\mathbf{G}_{pr}\,\mathbf{X}$$
$$\tilde{\mathbf{B}} = \mathbf{X}^T\mathbf{TB} \qquad \tilde{\mathbf{L}} = \mathbf{X}^T\mathbf{L} \tag{7}$$

$$\begin{aligned} \tilde{\mathbf{C}}\dot{\tilde{\mathbf{x}}}_q &= -\tilde{\mathbf{G}}\tilde{\mathbf{x}}_q + \mathbf{B}\mathbf{u}_p \\ \mathbf{i}_p &= \tilde{\mathbf{L}}^T\dot{\tilde{\mathbf{x}}}_q \end{aligned} \tag{8}$$

It was shown that the system in (8) was a passive reduced-order model, essentially because $\mathbf{G}_{pr}$ and $\mathbf{C}_{pr}$ were positive semi-definite [6]. The contents of $\mathbf{X}$ did not affect the passivity proof, thus providing us the flexibility to choose any $\mathbf{X}$ that is favorable for accuracy. Moreover, if $\mathbf{X}$ was selected as the basis for the Krylov space (5), the reduced order model would match at least the first k block moments, similar to the Arnoldi process.

Although this simple implementation proved itself to be useful in explaining the passivity and moment matching properties of the algorithm, it was not perfect for practical purposes. First, any loss in the orthogonality of $\mathbf{X}$ led to rank deficient $\tilde{\mathbf{G}}$ and $\tilde{\mathbf{C}}$, hence close to zero eigenvalues, resulting in very large negative or positive poles. Second, the explicit multiplications with $\mathbf{X}$ and the inversion of $\tilde{\mathbf{G}}$ injected unnecessary noise into the process.

3. Arnoldi and Lanczos Process Connections

In order to come up with a practical PRIMA algorithm, we first derive some theoretical connections between other Krylov space methods and PRIMA. Using the connections between Arnoldi, Lanczos and PRIMA system matrices, we can establish a practical framework for practically passive RLC circuit reduction.

3.1 Arnoldi and PRIMA System Matrices

Defining

$$\tilde{\mathbf{A}} \equiv -\tilde{\mathbf{G}}^{-1}\tilde{\mathbf{C}} \qquad \tilde{\mathbf{R}} \equiv \tilde{\mathbf{G}}^{-1}\tilde{\mathbf{B}}, \tag{9}$$

the reduced system computed using PRIMA can be formulated as

$$\begin{aligned} \tilde{\mathbf{A}}\dot{\tilde{\mathbf{x}}}_q &= \tilde{\mathbf{x}}_q - \tilde{\mathbf{R}}\mathbf{u}_p \\ \mathbf{i}_p &= \tilde{\mathbf{L}}^T\dot{\tilde{\mathbf{x}}}_q \end{aligned} \tag{10}$$

where $\mathbf{i}_p$ and $\mathbf{u}_p$ are the port currents and voltages respectively. Here we assumed that the macromodel had N ports and the order of reduction was q, therefore the approximation matched at least $\left\lfloor \frac{q}{N} \right\rfloor$ block moments at the ports.

From the standard Arnoldi process [3], we have the relation:

$$\mathbf{AX} = \mathbf{XH} + \mathbf{X}_l \tag{11}$$

$$\mathbf{X}_l = X_{last}\begin{bmatrix} \mathbf{0} & \mathbf{0} & \ldots & \mathbf{I} \end{bmatrix} \tag{12}$$

In (11), $\mathbf{H} \in \Re^{qxq}$ is the reduced-order block upper Hessenberg matrix and $X_{last} \in \Re^{nxN}$ is the last block Krylov vectors computed by the algorithm. Notice that only the last N columns of $\mathbf{X}_l \in \Re^{nxq}$ are nonzero.

Next, we can derive the relation between $\mathbf{H}$ and $\tilde{\mathbf{A}}$, hence the algebraic connection between PRIMA and Arnoldi system matrices. The usefulness of this relation will be apparent in the following sections. Multiplying (11) with $\mathbf{X}^T\mathbf{TG}$ and using (6), we obtain

$$-\mathbf{X}^T\mathbf{TCX} = \mathbf{X}^T\mathbf{TGXH} + \mathbf{X}^T\mathbf{TGX}_l. \tag{13}$$

Observing the relations in (4), (7) and multiplying each side in (13) by $\tilde{\mathbf{G}}^{-1}$ reveals the connection:

$$\tilde{\mathbf{A}} = -\tilde{\mathbf{G}}^{-1}\tilde{\mathbf{C}} = \mathbf{H} + \tilde{\mathbf{G}}^{-1}\mathbf{X}^T\mathbf{G}_{pr}\mathbf{X}_l \tag{14}$$

Only the last N columns of $\tilde{\mathbf{G}}^{-1}\mathbf{X}^T\mathbf{G}_{pr}\mathbf{X}_l \in \Re^{qxq}$ is nonzero because of the properties of $\mathbf{X}_l$. The interpretation of (14) is that PRIMA system matrix is indeed the Arnoldi system matrix with a perturbation on the last N columns (Fig.1a), when

$\mathbf{X}$ is obtained from an Arnoldi process.

3.2 Lanczos and PRIMA System Matrices

The Krylov space used in the PRIMA can be obtained from a Lanczos process too. The Lanczos governing equations [5] are:

$$\mathbf{A}\mathbf{V}_q = \mathbf{V}_q\mathbf{T}_q + \mathbf{v}_{q+1}\rho_{q+1}\begin{bmatrix}\mathbf{0} & \dots & \mathbf{I}\end{bmatrix} \tag{15}$$

$$\mathbf{A}^H\mathbf{W}_q = \mathbf{W}_q\tilde{\mathbf{T}}_q + \mathbf{w}_{q+1}\eta_{q+1}\begin{bmatrix}\mathbf{0} & \dots & \mathbf{I}\end{bmatrix} \tag{16}$$

We can replace $\mathbf{X}$ with $\mathbf{V}_q$ from (15) and obtain a PRIMA reduced order model from (7) [10]. Following a similar algebra as in Section 3.1, we obtain this relation between Lanczos and PRIMA system matrices:

$$\tilde{\mathbf{A}} = -\tilde{\mathbf{G}}^{-1}\tilde{\mathbf{C}} = \mathbf{T}_q + \tilde{\mathbf{G}}^{-1}\mathbf{X}^T\mathbf{G}_{pr}(\mathbf{v}_{q+1}\rho_{q+1}\begin{bmatrix}\mathbf{0} & \dots & \mathbf{I}\end{bmatrix}) \tag{17}$$

Since $\mathbf{T}_q$ is a tridiagonal matrix, $-\tilde{\mathbf{G}}^{-1}\tilde{\mathbf{C}}$ is a tridiagonal matrix with a modification for the last N columns (Fig.1b), when $\mathbf{X}$ is obtained using a Lanczos process.

3.3 Symmetric Case

When formulated in certain ways, RC circuit system matrices show useful symmetry properties which can be exploited by the underlying model order reduction technique. In a modified nodal analysis (MNA) based *impedance* formulation, $\mathbf{G}$ and $\mathbf{C}$ matrices are symmetric and positive definite. Therefore, we can use the Cholesky decomposition $\mathbf{R}^T\mathbf{R} = \mathbf{G}$. Let $\mathbf{J} = \mathbf{R}^{-1}$ and we can obtain this symmetric formulation:

$$\begin{aligned}\mathbf{J}^T\mathbf{C}\,\mathbf{J}\dot{\mathbf{x}}_n &= -\mathbf{x}_n + \mathbf{J}^T\mathbf{B}\,\mathbf{i}_p\\ \mathbf{u}_p &= \mathbf{L}^T\mathbf{J}\,\mathbf{x}_n\end{aligned} \tag{18}$$

where the system matrix $\mathbf{J}^T\mathbf{C}\,\mathbf{J}$ is symmetric and positive definite. Applying Arnoldi process to (18) produces a block tridiagonal $\mathbf{H}$ and matches $2q$ block moments for a qth order system [5], therefore resulting in a Padé approximation. Hence, Lanczos process and Arnoldi process produce the same reduced order matrices for the system in (18). Interestingly for this case, the modification to $\mathbf{H}$ in (14) becomes zero since $\mathbf{X}^T\mathbf{X} = \mathbf{I}$ and $\mathbf{X}^T\mathbf{X}_l = \mathbf{0}$ by construction of the Arnoldi algorithm. Therefore for (18), PRIMA, Arnoldi and Lanczos processes yield the same reduced order matrices. Similar symmetric formulations are also possible for LC and RL circuits [11].

A practical problem remains, however, for RC trees with no resistive path to ground. For the impedance modeling of such circuits, where current sources are connected to the ports and voltages at the ports are measured, $\mathbf{G}$ is not invertible. This practical problem is overlooked in the literature because of the possibility of avoiding the direct inversion of $\mathbf{G}$ by frequency shifting [12]. Shifting the frequency is equivalent to transforming $\mathbf{G}$ into $\mathbf{G} + s_0\mathbf{C}$, which is invertible for RC trees. Unfortunately, this shifting increases the matrix factorization complexity, and destroys the potential for path tracing.

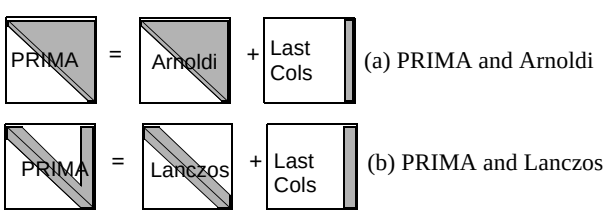

FIGURE 1: Relations of PRIMA and other Krylov space methods

4. PRIMA: A practical implementation

Similar to the original PRIMA implementation, the practical implementation consists of three stages as explained in the following subsections.

4.1 Stage 1: Finding the Krylov subspace

The Krylov subspace is the moment subspace of the system. Since moments of the circuit are invariant with respect to the circuit formulation, we can use the non-definite, but symmetric $\mathbf{G}$ matrix (rather than $\mathbf{G}_{pr}$) to obtain easier and better inversion. A simple numerically robust scheme to compute this subspace is via using the modified Gram-Schmidt orthogonalization procedure [8]. In this algorithm, after a moment vector is computed, the previous moment components are subtracted, therefore eliminating the bias of low order moments. To increase the orthogonality robustness, we can use multiple passes of orthogonalization [8]. A simple algorithm is presented in Fig.2. An example that

$\begin{bmatrix}\mathbf{X}_0, H_{1,0}\end{bmatrix} = qr(\mathbf{G}^{-1}\mathbf{B})$
for k = 1 to qn
  $\mathbf{X}_k = \mathbf{G}^{-1}\mathbf{C}\mathbf{X}_{k-1}$
  for np = 1 to NumberOfPasses
    for i = 1 to k
      $\Delta = \mathbf{X}_{i-1}^T\mathbf{X}_k$
      $\mathbf{X}_k = \mathbf{X}_k - \mathbf{X}_i\Delta$
      $H_{i,k} = H_{i,k} + \Delta$
  $\begin{bmatrix}\mathbf{X}_k, H_{k+1,k}\end{bmatrix} = qr(\mathbf{X}_k)$

$$\mathbf{X} = \begin{bmatrix}\mathbf{X}_0 & \dots & \mathbf{X}_{qn-1}\end{bmatrix} \text{ and } \mathbf{H} = \begin{bmatrix}H_{1,1} & \cdots & \\ \vdots & \ddots & \\ & & H_{q,q}\end{bmatrix}$$

FIGURE 2: Simple Krylov space computation scheme

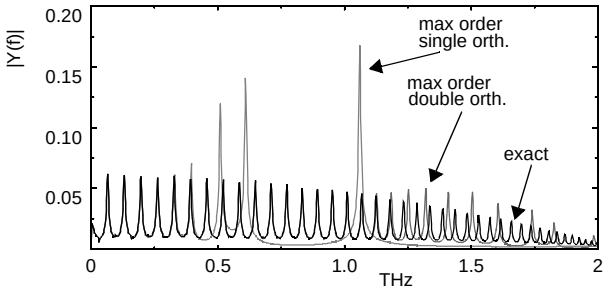

FIGURE 3: Improvement from using double orthogonalization in obtaining the Krylov space.

shows the improvement from using double orthogonalization (NumberOfPasses = 2) is given in Fig.3. The maximum order that can be reached by single orthogonalization is 48 (after which the Krylov vectors loose orthogonality), whereas it reaches to 128 with the use of double orthogonalization. The other example is taken from a four port PEEC circuit (Fig.4) with a dense *900x900* $\mathbf{C}$ matrix. The orthogonality of the Krylov space for the same example had weakened after 50 iterations with the single orthogonalization pass thereby resulting in numerically unstable reduced order models. However, it is demonstrated that the entire frequency range has been captured with the use of double pass orthogonalization, even with the expansion about s=0.

Double orthogonalization should be used when a very high order approximation is required. Such circuits are typically large RLC systems that take substantial amount of extraction time, therefore the extra cost with the use of multiple pass orthogonalization is relatively negligible.

We should emphasize that there are multiple ways of finding the Krylov subspace. It is indeed important to use a circuit type specific implementation. For example, a J-symmetric MPVL was used to generate the subspace and $\mathbf{H}$ matrix in [10].

In some applications, multipoint expansions can be tried. There has been extensive work in this field [13, 14]. An expansion at the frequency s_0 is simply finding the moments from

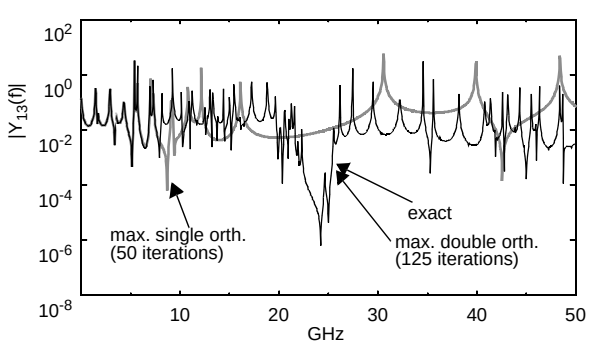

FIGURE 4: Limits of order reduction with different Krylov space construction methods demonstrated on a multiport PEEC circuit

$$\mathbf{X}_k = (\mathbf{G} + s_0\mathbf{C})^{-1}\mathbf{C}\mathbf{X}_{k-1}. \tag{19}$$

A simple extension of the basic Krylov space finding algorithm lets us to incorporate moments from different expansion points into $\mathbf{X}$. Difficulties arise when s_0 is a complex number, because of the involvement of complex algebra. It is possible to get rid of complex numbers by including the moments around $\overline{s_0}$ into $\mathbf{X}$ and exploiting the fact that the moments around s_0 will be conjugates of the moments around $\overline{s_0}$. Finding optimal expansion points, we have to mention, still remains an open problem. Moreover, $\mathbf{G} + s_0\mathbf{C}$ easily becomes dense for PEEC circuits, prohibiting the feasibility of the inversion in (19). We have observed that there is rarely a need for multipoint expansions with the use of double orthogonalization for Krylov vectors generated about *s=0*.

4.2 Stage 2: Computing the PRIMA matrices

Having $\mathbf{X}$ and $\mathbf{H}$ ready from stage 1, we can easily find the PRIMA matrices. Using (14) and $\tilde{\mathbf{G}}^{-1}\tilde{\mathbf{B}} = \mathbf{X}^T\mathbf{R}$ [6] gives the reduced order system as in (10) where

$$\begin{aligned} \tilde{\mathbf{A}} &= \mathbf{H} + (\mathbf{X}^T\mathbf{G}_{pr}\mathbf{X})^{-1}\mathbf{X}^T\mathbf{G}_{pr}\mathbf{X}_l \\ \tilde{\mathbf{R}} &= \mathbf{X}^T\mathbf{R} \qquad \tilde{\mathbf{L}} = \mathbf{X}^T\mathbf{L} \end{aligned} \tag{20}$$

4.3 Stage 3: Diagonalization

$\tilde{\mathbf{A}}$ in (20) is typically a block upper Hessenberg matrix. This presents storage and simulation run-time problems. The storage of a block upper Hessenberg matrix is $(\lfloor q/N \rfloor^2 + \lfloor q/N \rfloor)(N^2/2)$. By applying any eigendecomposition routine on $\tilde{\mathbf{A}}$, we can obtain

$$\tilde{\mathbf{A}} = \mathbf{S}\Lambda\mathbf{S}^{-1} \tag{21}$$

where Λ is a diagonal matrix that has at most *2q* real values. Indeed, the fact that $\tilde{\mathbf{A}}$ is an upper Hessenberg matrix can be exploited to use a better and more efficient eigendecomposition.

Since $\tilde{\mathbf{A}}$ is a real matrix, any complex eigenvalue or eigenvector has its conjugate. Therefore, we can use real $\mathbf{S}$ and Λ matrices by these simple transformations:

$$\mathbf{S}_r = \mathbf{S}\,\mathbf{P}^{-1} \text{ and } \Lambda_r = \mathbf{P}\Lambda\mathbf{P}^{-1} \tag{22}$$

$$\text{where } \tilde{\mathbf{A}} = \mathbf{S}_r\Lambda_r\mathbf{S}_r^{-1} \tag{23}$$

and $\mathbf{S}_r, \Lambda_r \in \Re^{qxq}$. $\mathbf{P} \in C^{qxq}$ is the transformation matrix that can be defined as

if $\Lambda_{i,i}$ is real, $\mathbf{P}_{i,i} = 1$,

if $\Lambda_{i,i} = \overline{\Lambda}_{i+1,i+1}$, $P_{i:i+1,i:i+1} = \begin{bmatrix} 1 & 1 \\ j & -j \end{bmatrix}$.

Hence, Λ_r will contain *2x2* blocks on the diagonal for complex eigenvalues, and *1x1* blocks for the real eigenvalues.

As a result, we have the reduced order system as:

$$\dot{\tilde{\mathbf{z}}}_q = \Lambda_r^{-1}\tilde{\mathbf{z}}_q - \Lambda_r^{-1}\mathbf{S}_r^{-1}\tilde{\mathbf{R}}\mathbf{u}_p$$
$$\mathbf{i}_p = \tilde{\mathbf{L}}^T \mathbf{S}_r \dot{\tilde{\mathbf{z}}}_q \tag{24}$$

Equation (24) characterizes a macromodel that can be directly inserted into any SPICE MNA matrix for simulation with nonlinear drivers. Equivalently, it can be used to synthesize a reduced-order circuit.

5. Convergence Criterion

The underlying moment matching mechanism in model order reduction techniques guarantees that the approximate transfer function captures the exact transfer function accurately in a radius f_r around the expansion frequency, f_0. As the order of approximation (q) increases, f_r increases as well; nevertheless the relation between f_r and q is not obvious. This nondeterminism in choosing the order of approximation renders model order reduction techniques impractical at times. It is desirable to find an error criterion for any approximation methodology to control the amount of error. However, there lies a fundamental problem: Knowing the error exactly or fairly accurately, requires the computation of the original system, which is not possible. Therefore any approximate error measure that is affordable is not accurate enough to be used as a direct measure for determining the order of approximation.

In this section, an approximate error measure is derived for PRIMA. It is assumed that the moments are found from expansions around zero for simplicity of the derivations, however the same logic applies to multipoint expansions. This error measure will be demonstrated as a good convergence criterion.

Following the algebra similar to that in [9], exact error of PRIMA transfer function is derived in Appendix A as

$$\mathbf{E}(s) = \mathbf{L}^T(\mathbf{I} - s\mathbf{A})^{-1} s\left(\mathbf{X}\tilde{\mathbf{G}}^{-1}\mathbf{X}^T\mathbf{G}_{pr}\mathbf{X}_l - \mathbf{X}_l\right)(\mathbf{I} - s\tilde{\mathbf{A}})^{-1}\mathbf{X}^T\mathbf{R} \tag{25}$$

In [9], $\left|(\mathbf{I} - s\mathbf{A})^{-1}\right|$ is replaced by $1/(1 - |s|\|\mathbf{A}\|)$ since

$$\left|(\mathbf{I} - s\mathbf{A})^{-1}\right| \le \frac{1}{1 - |s|\|\mathbf{A}\|} \text{ for } |s| < 1/\|\mathbf{A}\|. \tag{26}$$

However, the condition in (26) dictates a very narrow region for typical high frequency circuit applications. Instead, we choose to replace $(\mathbf{I} - s\mathbf{A})^{-1}$ in (25) with $\mathbf{X}(\mathbf{I} - s\tilde{\mathbf{A}})^{-1}\mathbf{X}^T$. Although this is not a bound, it is very useful in determining the convergence behavior. Therefore the approximate error measure becomes

$$\tilde{\mathbf{E}}(s) = \mathbf{L}^T\mathbf{X}(\mathbf{I} - s\tilde{\mathbf{A}})^{-1}\mathbf{X}^T s\left(\mathbf{X}\tilde{\mathbf{G}}^{-1}\mathbf{X}^T\mathbf{G}_{pr}\mathbf{X}_l - \mathbf{X}_l\right)(\mathbf{I} - s\tilde{\mathbf{A}})^{-1}\mathbf{X}^T\mathbf{R}$$

Observe that $\mathbf{X}^T\mathbf{X}_l = \mathbf{0}$ and $\mathbf{X}^T\mathbf{X} = \mathbf{I}$ as a property of the Krylov space generation. In addition, the use of (23) gives the approximate error measure for PRIMA:

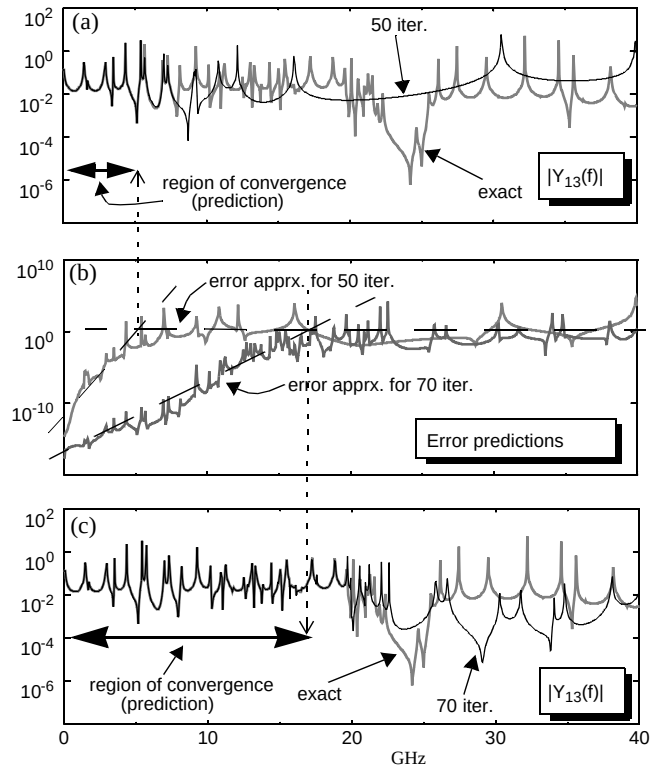

FIGURE 5: Demonstration of the convergence criteria based on the error measure.

$$\tilde{\mathbf{E}}(s) = \mathbf{L}^T\mathbf{X}\mathbf{S}_r(\mathbf{I} - s\Lambda)^{-1} \cdot$$
$$s\left(\mathbf{S}_r^{-1}\tilde{\mathbf{G}}^{-1}\mathbf{X}^T\mathbf{G}_{pr}\mathbf{X}_l\mathbf{S}_r\right)(\mathbf{I} - s\Lambda)^{-1}\mathbf{S}_r^{-1}\mathbf{X}^T\mathbf{R} \tag{27}$$

The computational expense in evaluating $\tilde{\mathbf{E}}(s)$ at several frequency points is very small because $(\mathbf{I} - s\Lambda)$ is a diagonal matrix. At a specific order of approximation, equation (27) can be used to estimate the region of convergence.

An example is the PEEC circuit that was used in Fig.4. In Fig.5, the use of approximate error measure (27) to understand the region of convergence, is shown. In Fig.5b, (27) is plotted with respect to the frequency for approximations that match 50 and 70 moments. As displayed, 50 moments around s=0 reaches up to 5GHz (Fig.5a) and 70 moments around s=0 converges up to 18 GHz (Fig.5c). In both cases, our error prediction successfully predicts the region of convergence.

6. Conclusion

In this paper, we have demonstrated a practically passive PRIMA implementation with an error checking mechanism. It is shown that it is possible to employ many Krylov space techniques, such as multi-point expansions and Lanczos process within the framework of PRIMA reduction to achieve passive and yet accurate macromodels.

Appendix A

In this appendix, we derive the exact error measure for the matrix transfer function obtained using PRIMA.

Multiplying (20) by $\mathbf{X}$ and rearranging terms yields

$$\mathbf{X}\,\mathbf{H} = \mathbf{X}\tilde{\mathbf{A}} - \mathbf{X}\tilde{\mathbf{G}}^{-1}\mathbf{X}^T\mathbf{G}_{pr}\mathbf{X}_l \tag{28}$$

Replacing $\mathbf{XH}$ in (11) with (28) and premultiplying by s, we obtain

$$s\mathbf{A}\mathbf{X} = s\mathbf{X}\tilde{\mathbf{A}} - s\mathbf{X}\tilde{\mathbf{G}}^{-1}\mathbf{X}^T\mathbf{G}_{pr}\mathbf{X}_l + s\mathbf{X}_l \tag{29}$$

Subtracting each side in (29) from $\mathbf{X}$ gives

$$(\mathbf{I} - s\mathbf{A})\mathbf{X} = \mathbf{X}(\mathbf{I} - s\tilde{\mathbf{A}}) + s\left(\mathbf{X}\tilde{\mathbf{G}}^{-1}\mathbf{X}^T\mathbf{G}_{pr}\mathbf{X}_l - \mathbf{X}_l\right) \tag{30}$$

It follows that

$$\begin{aligned}\mathbf{X}(\mathbf{I} - s\tilde{\mathbf{A}})^{-1} = {} & (\mathbf{I} - s\mathbf{A})^{-1}\mathbf{X} + \\ & (\mathbf{I} - s\mathbf{A})^{-1}s\left(\mathbf{X}\tilde{\mathbf{G}}^{-1}\mathbf{X}^T\mathbf{G}_{pr}\mathbf{X}_l - \mathbf{X}_l\right)(\mathbf{I} - s\tilde{\mathbf{A}})^{-1}\end{aligned} \tag{31}$$

$$\begin{aligned}\mathbf{L}^T\mathbf{X}(\mathbf{I} - s\tilde{\mathbf{A}})^{-1}\mathbf{X}^T\mathbf{R} = {} & \mathbf{L}^T(\mathbf{I} - s\mathbf{A})^{-1}\mathbf{X}\mathbf{X}^T\mathbf{R} + \\ & \mathbf{L}^T(\mathbf{I} - s\mathbf{A})^{-1}s\left(\mathbf{X}\tilde{\mathbf{G}}^{-1}\mathbf{X}^T\mathbf{G}_{pr}\mathbf{X}_l - \mathbf{X}_l\right)(\mathbf{I} - s\tilde{\mathbf{A}})^{-1}\mathbf{X}^T\mathbf{R}\end{aligned} \tag{32}$$

Since $\mathbf{X}\mathbf{X}^T\mathbf{R} = \mathbf{R}$ [6], and the matrix transfer functions are defined as

$$\tilde{\mathbf{H}}(s) = \mathbf{L}^T\mathbf{X}(\mathbf{I} - s\tilde{\mathbf{A}})^{-1}\mathbf{X}^T\mathbf{R}, \tag{33}$$

$$\mathbf{H}(s) = \mathbf{L}^T(\mathbf{I} - s\mathbf{A})^{-1}\mathbf{R}, \tag{34}$$

exact error of PRIMA transfer function is given as

$$\begin{aligned}\mathbf{E}(s) = {} & \tilde{\mathbf{H}}(s) - \mathbf{H}(s) = \\ & \mathbf{L}^T(\mathbf{I} - s\mathbf{A})^{-1}s\left(\mathbf{X}\tilde{\mathbf{G}}^{-1}\mathbf{X}^T\mathbf{G}_{pr}\mathbf{X}_l - \mathbf{X}_l\right)(\mathbf{I} - s\tilde{\mathbf{A}})^{-1}\mathbf{X}^T\mathbf{R}\end{aligned} \tag{35}$$

References

[1] L. T. Pillage and R. A. Rohrer, “Asymptotic waveform evaluation for timing analysis”, *IEEE Trans. Computer-Aided Design*, vol. 9, no. 4, pp. 352-366, Apr. 1990.

[2] P. Feldmann and R. W. Freund, “Efficient linear circuit analysis by Padé approximation via the Lanczos process”, *IEEE Trans. on CAD*, vol. 14, pp. 639-649, May 1995

[3] L. M. Silveira, M. Kamon and J. White, “Efficient reduced-order modeling of frequency-dependent coupling inductances associated with 3-D interconnect structures”, *IEEE/ACM Proc. DAC*, pp. 376-380, Jun. 1995

[4] E. J. Grimme, “Krylov projection methods for model reduction”, Ph.D. dissertation, Univ. Illinois, Urbana-Champaign, 1997

[5] D. L. Boley, “Krylov space methods on state-space control models”, *Circuits Syst. Signal Process*. vol.13, no.6, 1994

[6] A. Odabasioglu, M. Celik, and L. T. Pileggi, “PRIMA: Passive reduced-order interconnect macromodeling algorithm”, *IEEE Trans. on CAD*, vol. 17, no. 8, pp. 645-654, Aug. 1998

[7] E. Chiprout, "An error bound in interconnect simulation using PRIMA", *IEEE Workshop on Signal Propagation on Interconnects*, 1998

[8] Yousef Saad, *Iterative Methods For Sparse Linear Systems*, PWS Pub. Co., Jul. 1996

[9] Z. Bai, R. D. Slone, W. T. Smith, and Q. Ye, “Error bound for reduced system model by Padé approximation via the Lanczos process”, *IEEE Trans. on CAD*, vol. 18, no. 2, Feb. 1999

[10]R. W. Freund, “Passive reduced-order models for interconnect simulation and their computation via Krylov-subspace algorithms”, *IEEE/ACM Proc. DAC*, Jun. 1999

[11]J. E. Bracken, “Passive modelling of linear interconnect networks”, *Technical Report*, Dept. of ECE, Carnegie Mellon University, 1995

[12]R. W. Freund and P. Feldmann, “Reduced order modeling of large passive linear circuits by means of the SyPVL algorithm”, *IEEE/ACM Proc. ICCAD*, pp. 280-287, Nov. 1996

[13]I. M. Elfadel, and D. D. Ling, “A block rational Arnoldi algorithm for multipoint passive model-order reduction of multiport RLC networks”, *IEEE/ACM Proc. ICCAD*, pp.66-71, Nov. 1997

[14]Q. Yu, J. M. L. Wang, and E. S. Kuh, “Passive multipoint moment matching model order reduction algorithm on multiport distributed interconnect networks”, *IEEE Trans. on Circuits and Systems-I*, vol. 46, no. 1, pp.140-160, Jan. 1999